crystals

MDPI

Article

Study on the Effect of Different Factors on the Change of the Phosphorus-Rich Phase in High Phosphorus Steel Slag

Zhongliang Wang, Yanping Bao *, Dazhi Wang, Chao Gu and Min Wang

State Key Laboratory of Advanced Metallurgy, University of Science and Technology Beijing, Xueyuan Road 30#, Haidian District, Beijing 100083, China; b20200576@xs.ustb.edu.cn (Z.W.); b20180528@xs.ustb.edu.cn (D.W.); guchao@ustb.edu.cn (C.G.); wangmin@ustb.edu.cn (M.W.)

* Correspondence: baoyp@ustb.edu.cn

Abstract: With the use of high phosphorus iron ore, there is a large amount of high phosphorus steel slag formed, which is difficult to handle. How to separate the elemental phosphorus has become a key issue in the secondary utilization of steel slag. Experiments found that there were distinct phosphorus-rich phases, iron-rich phases and matrix phases in the high-phosphorus steel slag cooled with the furnace. In this study, the effects of heat treatment conditions and slag basicity on the P_2O_5 content, as well as the size of the phosphorus-rich phase were investigated. Taking all factors into consideration, the optimal experimental conditions were determined as the holding temperature and time of 1350 °C and 60 min, respectively, and the slag basicity of 1.8. At this time, the P_2O_5 content in the phosphorus-rich phase reached 24.2%, and the average size of the phosphorus-rich phase was 63.51 μm. The phosphorus-rich phase is separated by crushing and magnetic separation for making phosphate fertilizer, and the residual steel slag is used again for steelmaking, which enables the realization of the resource utilization of high phosphorus steel slag.

Keywords: high phosphorus steel slag; phosphorus-rich phase; holding temperature; binary basicity; holding time

Citation: Wang, Z.; Bao, Y.; Wang, D.; Gu, C.; Wang, M. Study on the Effect of Different Factors on the Change of the Phosphorus-Rich Phase in High Phosphorus Steel Slag. *Crystals* **2022**, *12*, 1030. https://doi.org/10.3390/cryst12081030

Academic Editors: Jie Dang and Zhiyuan Chen

Received: 17 June 2022
Accepted: 23 July 2022
Published: 25 July 2022

1. Introduction

Iron ore is an indispensable non-renewable resource in steel production, and with the continuous development of the iron and steel industry, the demand for iron ore is increasing, resulting in a decline in the reserves of high-grade iron ore year by year. It is urgent to develop and utilize complex refractory ores, especially the huge amount of high phosphate ores [1–4]. However, in the iron and steel production process, sintering and blast furnace smelting cannot dephosphorize, and enough slagging agent can only be added in the steelmaking process to make the composition of molten steel qualified [5,6]. Otherwise, if the phosphorus content is high, the steel will be too brittle at low temperature, seriously reducing its use performance [7]. The use of high-phosphate iron ore is bound to increase the content of phosphorus in slag, affecting the recycling times of slag in steelmaking, thus generating a greater burden on slag treatment. The stock of unused steel slag in China has exceeded 300 million tons, while about 100 million tons of new steel slag is produced each year, and the utilization rate is less than 50%. A large amount of steel slag is directly piled into slag mountains, occupying land resources and polluting soil and groundwater resources [8].

The current secondary reuse methods of steel slag mainly include use in the construction field, such as building materials, road paving, and cement production [9–11]. It is used in the agricultural field, for example, as fertilizers and soil conditioners to make full use of silicon, calcium, phosphorus and other elements in slag [12]. It is also used in iron and steel enterprises for magnetic separation to recover iron particles, as metallurgical flux [13,14]. Therefore, the efficient resource utilization of converter slag has become a hot issue concerning many scholars. Various reducing agents were used to reduce phosphorus from

steel slag in a hot state to complete gasification dephosphorization [15,16]. Several scholars studied the magnetic separation process of converter slag and achieved the purpose of recovering valuable elements from converter slag by adding different modifiers to the slag and using an optimal magnetic separation process [17–20]. In some studies, selective leaching of steel slag was carried out with acid solutions of different pH values, and it was found that the highest leaching rate of elements in the slag was calcium, followed by silicon and phosphorus, and the lowest was iron [21–23]. To realize the green cycle, Matsuura et al. creatively used seawater as the leaching solution, and found that the leaching rate of phosphorus decreased with the increase in the pH value of seawater, and the final effect was slightly inferior to that of an acid solution [24–26].

The phosphorus content in high-phosphorus steel slag is usually greater than 5%, and can even reach 10%, but the distribution of phosphorus elements in the slag obtained under actual production conditions is relatively scattered [27]. The molten iron needed to be dephosphorized below 1500 °C, which required that the content of CaO in the slag could not be too high. Thus, the basicity of high phosphorus steel slag was generally lower than 2. If the phosphorus can be further enriched, not only high phosphorus steel slag can be used as a new phosphorus source, but also the residue after separation and dephosphorization can be recycled many times. Studies have shown that phosphorus in steel slag mainly exists in $2CaO{\cdot}SiO_2$-$3CaO{\cdot}P_2O_5$ solid solution, and the theoretical solid solubility of P_2O_5 can reach more than 30% [28]. However, due to the basicity and cooling rate of steel slag, the actual solid solubility is generally lower than this value. In the basicity range of converter slag, the slag viscosity decreased with the increase in CaO content [29]. Moreover, after the converter slag pouring, the steel slag was usually sprayed with atomized water, resulting in rapid cooling [8]. Both hindered the migration of P_2O_5 and could not reach the optimal enrichment state before solidification. The components with high content in steel slag are calcium oxide and silica, and temperature and time will significantly affect the formation of $2CaO{\cdot}SiO_2$-$3CaO{\cdot}P_2O_5$ solid solution. Therefore, it is necessary to study the effect of different factors on the enrichment of phosphorus in high phosphorus steel slag to find favorable conditions and promote subsequent utilization of steel slag [30–33]. In this study, the CaO-SiO_2-Fe_2O_3-P_2O_5-MgO-MnO slag system synthesized in the laboratory was used as the research object, and the effects of different holding temperatures, binary basicity and holding time on the high phosphorus steel slag were investigated. Based on the influence of phosphorus enrichment behavior, the optimal conditions for controlling phosphorus enrichment were obtained, which provided a theoretical basis for realizing the resource utilization of high phosphorus steel slag.

2. Materials and Methods

2.1. Experimental Materials

In order to eliminate the interference of other impurities, the high phosphorus steel slag used in this experiment was prepared from analytically pure CaO, SiO_2, Fe_2O_3, P_2O_5, MgO, $MnCO_3$ chemical reagents, and the specific composition of the slag sample was shown in Table 1. The contents of fixed Fe_2O_3, P_2O_5, MgO and MnO in the six component slag system were 25%, 10%, 5% and 5%, respectively.

Table 1. Slag composition and heat treatment method in each experiment (wt.%).

NO.	CaO	SiO_2	Fe_2O_3	P_2O_5	MnO	MgO	R	Temperature/°C	Time/min
1	36.67	18.33	25	10	5	5	2	1400	30
2	36.67	18.33	25	10	5	5	2	1375	30
3	36.67	18.33	25	10	5	5	2	1350	30
4	36.67	18.33	25	10	5	5	2	1300	30
5	35.36	19.64	25	10	5	5	1.8	1350	30
6	33	22	25	10	5	5	1.5	1350	30
7	27.5	27.5	25	10	5	5	1	1350	30
8	35.36	19.64	25	10	5	5	1.8	1350	15
9	35.36	19.64	25	10	5	5	1.8	1350	45
10	35.36	19.64	25	10	5	5	1.8	1350	60

2.2. Experimental Methods

The 50 g of reagent prepared according to the composition requirements were thoroughly mixed in the mixer for 1 min, and each substance was uniformly dispersed without agglomeration. The mixture was placed in a magnesia crucible with a diameter of 60 mm and a height of 100 mm, which was then fed into a box furnace heated by silicon molybdenum rods, as shown in Figure 1a. The variables in this study were slag composition and heat treatment method, where the former was the ratio of CaO to SiO_2, that is, binary basicity, and the latter was mainly the holding temperature and holding time of the slag, that is, the heating system. Referring to the actual production data, the binary basicity in experiments 3, 5, 6, and 7 was set to 2, 1.8, 1.5, and 1 from high to low, and the rest of the variables were the same. The heating system adopted was shown in Figure 1b. First, it was heated from room temperature to 1500 °C and kept for 100 min to ensure that the high phosphorus steel slag was fully melted. Then, the holding temperature was adjusted in experiments 1, 2, 3, and 4, and the holding time was adjusted in experiments 5, 8, 9, and 10. Finally, it was cooled to room temperature with the furnace for sampling and analysis.

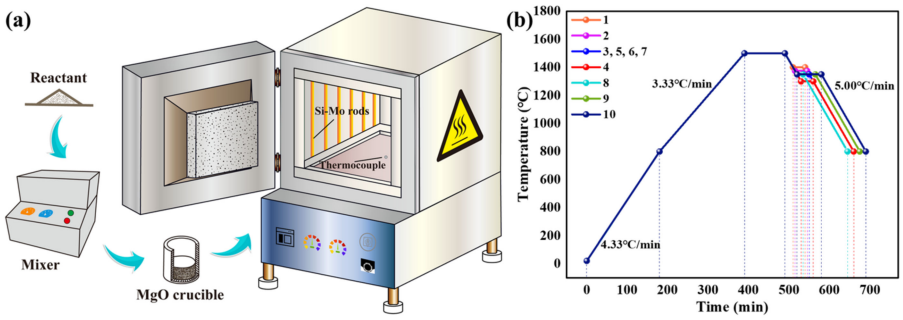

Figure 1. Experimental methods (**a**) schematic diagram of equipment, and (**b**) heating system.

2.3. Sample Analysis

Five slag samples were selected at equal intervals from the edge to the core of each crucible. These appropriately sized bulk samples were embedded in epoxy resin, after grinding, polishing and gold spraying, the morphology was observed under scanning electron microscopy (SEM; Pro-X, Phenom, Eindhoven, The Netherlands), and the micro-area composition was analyzed by energy dispersive X-ray spectrometry (EDS). The rest of the samples were broken below 0.074 mm and their phase composition was detected by powder X-ray diffraction that employed a scan rate of 10° min^{-1} from 10° to 90° with Cu Kα radiation (XRD; Smart-Lab, Rigaku, Tokyo, Japan). The SEM images of different positions in the same sample were processed and analyzed by ImageJ, in which the diameters of the phosphorus rich phase were counted. Further, the longest diagonal of the irregular shape was taken as the diameter of the phosphorus rich phase for the unified standard.

3. Results and Discussion

3.1. Pre-Experiment

The phase diagram of CaO-SiO_2-Fe_2O_3-P_2O_5-MgO-MnO slag system was drawn using Factsage 7.2. From Figure 2a, it could be seen that the theoretical phase composition of each component in the experiment was basically the same, and they were all in the primary zone of $Ca_5(PO_4)_2SiO_4$. The XRD analysis of all high phosphorus steel slag found that there was almost no difference in peak positions, but there was a slight difference in the peak intensity, indicating that the phase composition of the slag was exactly the same, but the proportions of each phase were different, which was also consistent with the research results of Ye et al. [14]. Figure 2b was a typical XRD pattern of the steel slag in this experiment, mainly including four phases: $CaSiO_3$, $Ca_5(PO_4)_2SiO_4$, $Ca_{2.87}Fe_{0.13}(SiO_3)_3$ and $Fe_4(PO_4)_2O$. As shown in Figure 2c, the steel slag showed obvious phase separation after cooling with the furnace, which could be divided into a phosphorus-rich phase, iron-rich phase and matrix phase, according to the composition in Table 2. The phosphorus-rich phase was gray–black, mostly distributed in irregular stripes and ellipses, and grew staggered with the matrix. The iron-rich phase was white, and there was an obvious sharp boundary with other phases. The matrix phase was gray, and its distribution characteristics changed with the changes of the former two. The elemental phosphorus was mainly distributed in the phosphorus-rich phase, with low content in the iron-rich and matrix phases. Therefore, in order to explore the enrichment law of phosphorus in steel slag, it was necessary to focus on the changes of the phosphorus-rich phase under different conditions, which is also the key content of this paper.

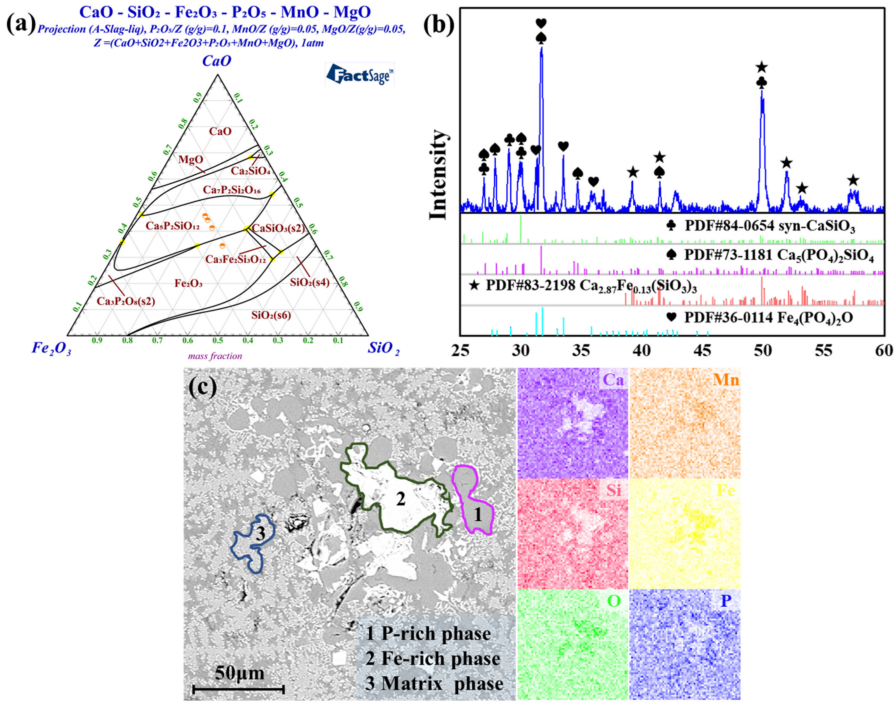

Figure 2. Phases of high phosphorus steel slag (**a**) phase diagram containing the composition of experimental slag (**b**) XRD patterns and (**c**) SEM and EDS micro-morphology.

Table 2. Typical composition of each phase of high phosphorus steel slag (wt.%).

Area	CaO	SiO_2	Fe_2O_3	MgO	MnO	P_2O_5
P-rich phase	50.0	25.6	0	5.1	0	19.3
	52.1	21.2	0	4.2	0	22.5
	50.7	22.3	0	4.6	0	22.4
Fe-rich phase	4.4	3.6	75.2	14.3	0	2.6
	4.6	4.1	75.4	13.5	0	2.4
	8.6	6.0	66.9	14.2	0	4.3
Matrix phase	34.4	38.3	9.5	12.0	0	5.8
	34.1	36.7	9.3	12.7	0	7.3
	33.8	37.8	9.2	13.0	0	6.2

3.2. Effects of Different Factors on Phosphorus-Rich Phase

3.2.1. Holding Temperature

Figure 3a–d showed the micro-morphology of high phosphorus steel slag at holding temperatures of 1400 °C, 1375 °C, 1350 °C and 1300 °C. The boundaries of phosphorus-rich phase, iron-rich phase and matrix phase were clear and could be intuitively identified. The effect of different holding temperatures on the phosphorus content in the phosphorus-rich phase was shown in Figure 3e. When the heat treatment temperature of high phosphorus steel slag was 1400 °C, the P_2O_5 content in the phosphorus-rich phase was the highest, reaching 22.8%. As the holding temperature decreased from 1400 °C to 1300 °C, the P_2O_5 content was only 15.4%. At 1375 °C and 1350 °C, there was little difference in P_2O_5 content of the phosphorus-rich phase, being 19.5% and 19.2%, respectively, between the maximum and minimum values. The effect of different holding temperatures on the average size of the phosphorus-rich phase is presented in Figure 3f. Due to the mutual annexation and growth of solid solutions, the size distribution of the phosphorus-containing phase was broad, and the method of taking the average value after a large number of statistics was used for description. During the holding process, the size of the phosphorus-rich phase decreased as the temperature decreased. When the holding temperature was 1400 °C, the average size of the phosphorus-rich phase was 46.37 μm. At 1375 °C, 1350 °C and 1300 °C, the size of the phosphorus-rich phase decreased to 36.14 μm, 25.96 μm and 20.95 μm, respectively. Therefore, during the cooling process of high phosphorus steel slag, the temperature was kept at about 1400 °C, which was beneficial to improve the enrichment effect of phosphorus in the slag.

3.2.2. Binary Basicity

As shown in Figure 4a–d, it was the micro-morphology of high phosphorus steel slag with the basicity of 2, 1.8, 1.5 and 1. In Figure 4e,f, the effect of different basicity on the P_2O_5 content, as well as the size of the phosphorus-rich phase, is presented. When the slag basicity was 2, the P_2O_5 content in the phosphorus-rich phase was 19.2%, and as the value decreased to 1.8, the P_2O_5 content in the phosphorus-rich phase increased to 21.6%. After the basicity reached 1.8, the continued increase adversely affected the enrichment of phosphorus in the steel slag. For the slag with basicities of 1.5 and 1, the P_2O_5 content in the phosphorus-rich phase was 20.7% and 13.8%, respectively. The decrease in basicity caused the P_2O_5 content in the phosphorus-rich phase to decrease rapidly. This was mainly because when the basicity of high-phosphorus steel slag was low, less $2CaO{\cdot}SiO_2$ phase was precipitated during the cooling process, resulting in poor phosphorus enrichment in the slag. Consequently, when the basicity was low (<1.8), it was beneficial to appropriately increase the basicity of steel slag for phosphorus enrichment. However, if the basicity was too high, a large amount of $3CaO{\cdot}SiO_2$ would be generated during the cooling process, and $3CaO{\cdot}SiO_2$ could not be infinitely co-soluble with $3CaO{\cdot}P_2O_5$, meanwhile, the viscosity of slag increased, which was not conducive to the migration of phosphorus, all of which affected the enrichment of phosphorus. In the box plot of Figure 4f, it was found that the size

of the phosphorus-rich phase decreased with the decreasing basicity of the high phosphorus steel slag. In particular, the average size of the phosphorus-rich phase rapidly decreased from 18.31 μm to 9.70 μm during the basicity of 1.5 to 1. After the basicity exceeded 1.5, the average size of the phosphorus-rich phase increased slowly, and the corresponding values were 21.30 μm and 25.96 μm when the basicity was 1.8 and 2. According to the above experimental results, controlling the basicity of steel slag between 1.5 and 1.8 was very beneficial to the enrichment of phosphorus.

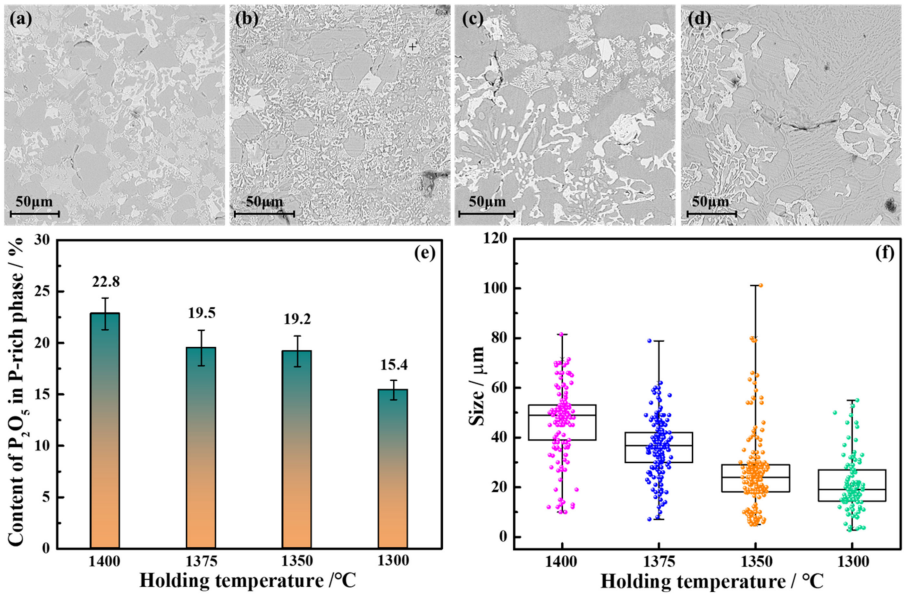

Figure 3. (**a**–**d**) Microscopic appearance of high phosphorus steel slag (**e**) P_2O_5 content and (**f**) size of phosphorus-rich phase under different holding temperatures.

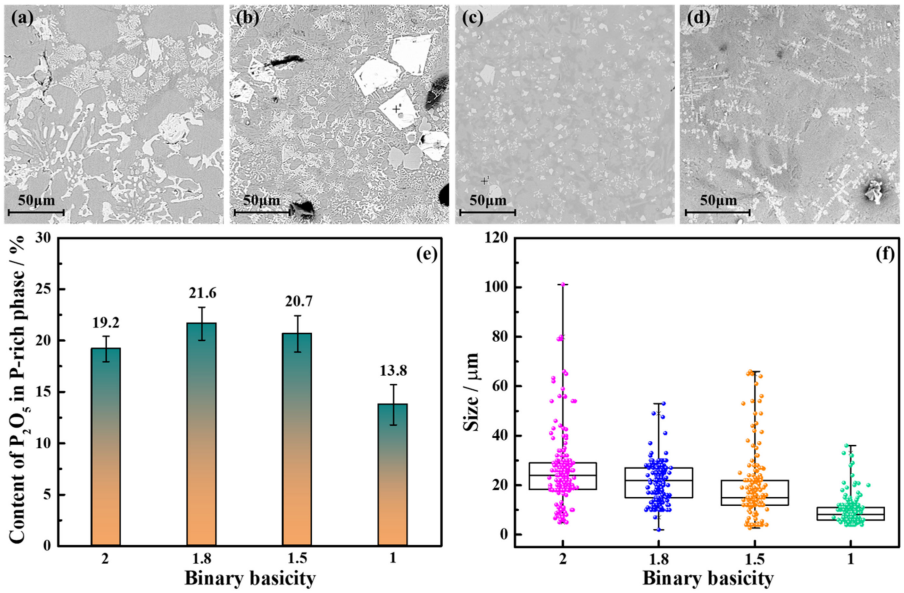

Figure 4. (**a**–**d**) Microscopic appearance of high phosphorus steel slag (**e**) P_2O_5 content and (**f**) size of the phosphorus-rich phase under different binary basicity.

3.2.3. Holding Time

The first two subsections determined the best heat treatment temperature and appropriate basicity of high phosphorus steel slag. In this section, the effect of holding time on the phosphorus-rich phase was mainly explored. Figure 5a–d showed the micro-morphology of high phosphorus steel slag when the basicity was 1.8, the holding temperature was

1350 °C and the holding time was 15 min, 30 min, 45 min and 60 min. As shown in Figure 5e, the P_2O_5 content in the phosphorus-rich phase increased significantly with the increase in holding time, especially in the process of holding for 15 min to 30 min, the increase value was the largest. However, when the holding time exceeded 30 min, the increase rate of P_2O_5 content in the phosphorus-rich phase became smaller. Through the statistical data in the box plot of Figure 4f, it was found that the phosphorus-rich phase size had the same change trend as the P_2O_5 content, but the difference was that the increase rate of the phosphorus-rich phase size increased greatly in the later stage of holding. The average size of the phosphorus-rich phase at 15 min of holding time was 17.16 μm. In the same 15 min interval after that, the size increased by 4.14 μm, 20.31 μm and 21.90 μm, respectively, reaching 21.30 μm, 41.61 μm and 63.51 μm. Considering the enrichment effect, controlling the holding time to 60 min was the best for the formation and growth of the phosphorus-rich phase. However, from the point of view of energy consumption, too high holding temperature and too long holding time increased heat dissipation and aggravated greenhouse gas emissions. As a consequence, these factors should be comprehensively considered in practical application, so as to obtain the best treatment conditions for high phosphorus steel slag.

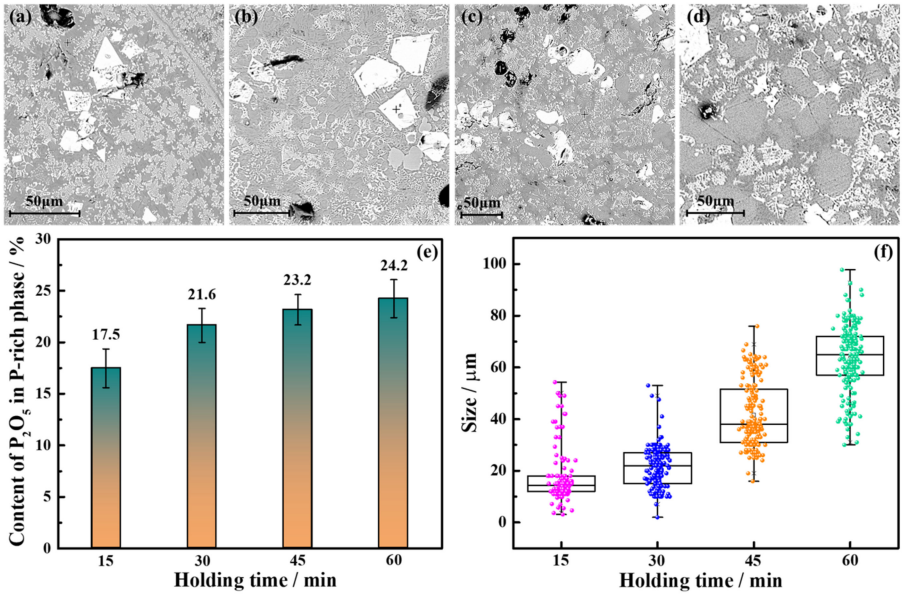

Figure 5. (**a**–**d**) Microscopic appearance of high phosphorus steel slag (**e**) P_2O_5 content and (**f**) size of phosphorus-rich phase under different holding times.

3.3. Mechanism Analysis

The precipitation of $Ca_5(PO_4)_2SiO_4$ from high phosphorus steel slag during cooling from steelmaking temperature to room temperature, as shown in Figure 6, could be divided into three steps. In the first step, Ca, Si and O in the slag formed easily crystallizable Ca_2SiO_4, which provided sufficient solid solution sites for the enrichment of P_2O_5. In the second step, free CaO and P_2O_5 diffused toward Ca_2SiO_4, forming a high concentration region around this crystal. In the third step, Ca_2SiO_4 combined with CaO and P_2O_5 to form $Ca_5(PO_4)_2SiO_4$ solid solution, which accumulated and grew continuously. It mainly involved the following two reactions:

$$2CaO + SiO_2 = Ca_2SiO_4 \quad (1)$$

$$\Delta G_1 = \Delta G_1^\theta + RT \ln Q_1 = \Delta G_1^\theta + RT \ln \frac{a_{Ca_2SiO_4}}{a_{CaO}^2 \cdot a_{SiO_2}} \quad (2)$$

$$Ca_2SiO_4 + 3CaO + P_2O_5 = Ca_2SiO_4 \cdot Ca_3(PO_4)_2 \quad (3)$$

$$\Delta G_2 = \Delta G_2^\theta + RT \ln Q_2 = \Delta G_2^\theta + RT \ln \frac{a_{Ca_2SiO_4 \cdot Ca_3(PO_4)_2}}{a_{Ca_2SiO_4} \cdot a_{CaO}^3 \cdot a_{P_2O_5}} \quad (4)$$

where ΔG_1 and ΔG_2 were the reaction Gibbs free energies of reaction (1) and (3). ΔG_1^θ and ΔG_2^θ were the standard reaction Gibbs free energies of reaction (1) and (3). Q_1 and Q_2 were the reaction quotients of reaction (1) and (3). a_{CaO}, $a_{P_2O_5}$, a_{SiO_2}, $a_{Ca_2SiO_4}$ and $a_{Ca_2SiO_4 \cdot Ca_3(PO_4)_2}$ were the activities of the corresponding substances, respectively. Among them, since the formed Ca_2SiO_4 and $Ca_5(PO_4)_2SiO_4$ were solid, both could be considered as pure substances with an activity of 1, so the Equations (2) and (4) could be simplified to (5) and (6).

$$\Delta G_1 = \Delta G_1^\theta + RT \ln Q_1 = \Delta G_1^\theta - RT \ln a_{CaO}^2 \cdot a_{SiO_2} \quad (5)$$

$$\Delta G_2 = \Delta G_2^\theta + RT \ln Q_2 = \Delta G_2^\theta - RT \ln a_{CaO}^3 \cdot a_{P_2O_5} \quad (6)$$

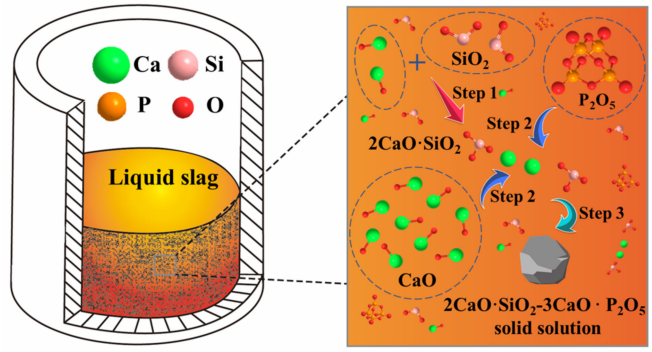

Figure 6. Formation mechanism diagram of $Ca_5(PO_4)_2SiO_4$.

Therefore, the direct influencing factors for the formation of phosphorus-rich phase in steel slag were the activities of CaO, SiO_2 and P_2O_5, and whether the above reactions could reach equilibrium. The holding temperature and basicity mainly affected the activity, while the holding time mainly affected the degree of reaction proceeding. When the holding temperature increased, the reactant activity increased, and at the same time, it could promote the positive reaction, and the P_2O_5 content and size of the phosphorus-rich phase increased. Binary basicity was the ratio of CaO and SiO_2 content in slag. Within a certain range, the larger the value, the higher the CaO content, and the higher the corresponding CaO activity, the more Ca_2SiO_4 and $Ca_5(PO_4)_2SiO_4$ were generated. However, the basicity could not continue to increase, when the CaO content in the slag was too high, as it would generate Ca_3SiO_5 that could not be infinitely co-soluble with P_2O_5. At this time, the fluidity of the slag also became poor, which was not conducive to the growth of the phosphorus-rich phase. The mass transfer in high phosphorus steel slag was relatively slow, and after the reaction, it took a long time for the aggregation of reactants and the growth of products. In the experiment, the law that the P_2O_5 content and size of the phosphorus-rich phase increased with the prolongation of the reaction time was obtained, which also confirmed this view.

4. Conclusions

In general, the high-phosphorus steel slag cooled with the furnace was mainly composed of a gray–black phosphorus-rich phase, white iron-rich phase and gray matrix phase. The phosphorus element mainly existed in the phosphorus-rich phase in the form of a $Ca_5(PO_4)_2SiO_4$ solid solution, and the P_2O_5 content in the other two phases was low. The heat treatment method and binary basicity had no effect on the occurring form of phosphorus but were able to change the P_2O_5 content and the size of the phosphorus-rich phase. Through experimentation, it was found that with the increase in holding temperature and holding time, the P_2O_5 content and size of the phosphorus-rich phase increased. The effect of basicity was different from these two. When the basicity was lower than 1.8, the increase in its value contributed to the enrichment of phosphorus. However, when the basicity

was higher than 1.8, the increase in its value could still slightly increase the size of the phosphorus-rich phase, and on the other hand, the P_2O_5 content was significantly reduced. Therefore, taking into account the phosphorus enrichment effect and the relatively low energy consumption, the optimal experimental conditions were determined as the holding temperature and time of 1350 °C and 60 min, respectively, and the slag basicity of 1.8. At this time, the P_2O_5 content in the phosphorus-rich phase reached 24.2%, and the average size of the phosphorus-rich phase was 63.51 μm. Based on these, the phosphorus-rich phase in the high-phosphorus steel slag can be used for the production of chemical fertilizers through magnetic separation and other means, and the remaining residues can be reused in the steelmaking process to realize the resource utilization of high phosphorus steel slag.

Author Contributions: Conceptualization, Z.W. and Y.B.; methodology, D.W.; software, M.W.; validation, Z.W., D.W. and C.G.; funding acquisition, Y.B. All authors have read and agreed to the published version of the manuscript.

Funding: This research was funded by the National Natural Science Foundation of China, grant number 51574019.

Institutional Review Board Statement: Not applicable.

Informed Consent Statement: Not applicable.

Data Availability Statement: Not applicable.

Conflicts of Interest: The authors declare no conflict of interest.

References

1. Sun, Y.; Zhang, Q.; Han, Y.; Gao, P.; Li, G. Comprehensive utilization of iron and phosphorus from high-phosphorus refractory iron ore. *JOM* **2018**, *70*, 144–149. [CrossRef]
2. Zhang, Y.; Xue, Q.; Wang, G.; Wang, J. Phosphorus-containing mineral evolution and thermodynamics of phosphorus vaporization during carbothermal reduction of high-phosphorus iron ore. *Metals* **2018**, *8*, 451. [CrossRef]
3. Sun, Y.; Li, Y.; Han, Y.; Li, Y. Migration behaviors and kinetics of phosphorus during coal-based reduction of high-phosphorus oolitic iron ore. *Int. J. Miner. Metall. Mater.* **2019**, *26*, 938–945. [CrossRef]
4. Wu, J.; Wen, Z.; Cen, M. Development of technologies for high phosphorus oolitic hematite utilization. *Steel Res. Int.* **2011**, *82*, 494–500.
5. Yang, W.; Yang, J.; Shi, Y.; Yang, Z.; Gao, F.; Zhang, R.; Ye, G. Effect of basicity on dephosphorization of hot metal with a low basicity slag at 1653 K. *Ironmak. Steelmak.* **2021**, *48*, 69–77. [CrossRef]
6. Zhou, W.; Han, Y.; Sun, Y.; Li, Y. Strengthening iron enrichment and dephosphorization of high-phosphorus oolitic hematite using high-temperature pretreatment. *Int. J. Miner. Metall. Mater.* **2020**, *27*, 443–453. [CrossRef]
7. Enzian, G. Some effects of phosphorus and nitrogen on the properties of low carbon steel. *JOM* **1950**, *2*, 346–353. [CrossRef]
8. Guo, J.; Bao, Y.; Wang, M. Steel slag in China: Treatment, recycling, and management. *Waste Manag.* **2018**, *78*, 318–330. [CrossRef]
9. Perez-Garcia, F.; Parron-Rubio, M.E.; Garcia-Manrique, J.M.; Rubio-Cintas, M.D. Study of the suitability of different types of slag and its influence on the quality of green grouts obtained by partial replacement of cement. *Materials* **2019**, *12*, 1166. [CrossRef]
10. Lee, J.; Choi, J.; Yuan, T.; Yoon, Y.; Mitchell, D. Comparing properties of concrete containing electric arc furnace slag and granulated blast furnace slag. *Materials* **2019**, *12*, 1371. [CrossRef]
11. Yüksel, İ. A review of steel slag usage in construction industry for sustainable development. *Environ. Dev. Sustain.* **2017**, *19*, 369–384. [CrossRef]
12. Gao, D.; Wang, F.; Wang, Y.; Zeng, Y. Sustainable utilization of steel slag from traditional industry and agriculture to catalysis. *Sustainability* **2020**, *12*, 9295. [CrossRef]
13. Varanasi, S.S.; More, V.M.R.; Rao, M.B.V.; Alli, S.R.; Tangudu, A.K.; Santanu, D. Recycling ladle furnace slag as flux in steelmaking: A review. *J. Sustain. Metall.* **2019**, *5*, 449–462. [CrossRef]
14. Ye, G.; Yang, J.; Zhang, R.; Yang, W.; Sun, H. Behavior of phosphorus enrichment in dephosphorization slag at low temperature and low basicity. *Int. J. Miner. Metall. Mater.* **2021**, *28*, 66–75. [CrossRef]
15. Wang, Z.; Bao, Y.; Wang, D.; Wang, M. Effective removal of phosphorus from high phosphorus steel slag using carbonized rice husk. *J. Environ. Sci.* **2023**, *124*, 156–164. [CrossRef]
16. Xue, Y.; Zhao, D.; Wang, S.; Li, C.; Guo, R. Phosphorus vaporization behaviour from converter slag. *Ironmak. Steelmak.* **2020**, *47*, 892–898. [CrossRef]
17. Lin, L.; Bao, Y.; Wang, M.; Zhou, H. Influence of Al_2O_3 modification on phosphorus enrichment in P bearing steelmaking slag. *Ironmak. Steelmak.* **2014**, *41*, 193–198. [CrossRef]

18. Wang, Z.; Shu, Q.; Sridhar, S.; Zhang, M.; Guo, M.; Zhang, Z. Effect of P_2O_5 and Fe_tO on the viscosity and slag structure in steelmaking slags. *Metall. Mater. Trans. B* **2015**, *46*, 758–765. [CrossRef]
19. Xie, S.; Wang, W.; Pan, Z.; Li, H.; Huang, D.; Du, y. Effect of Al_2O_3 on the melting, viscosity, and phosphorus distribution of CaO–SiO_2–Fe_2O_3–P_2O_5 slag system. *Steel Res. Int.* **2018**, *89*, 1700516. [CrossRef]
20. Yan, W.; Hao, Z.; Chen, W.; Li, J. Mixing effect of slag compositions and additives on crystallization of mold fluxes for Ti-bearing steels. *Steel Res. Int.* **2021**, *10*, 882–894. [CrossRef]
21. Teratoko, T.; Maruoka, N.; Shibata, H.; Kitamura, S. Dissolution behavior of dicalcium silicate and tricalcium phosphate solid solution and other phases of steelmaking slag in an aqueous solution. *High Temp. Mater. Process.* **2012**, *31*, 329–338. [CrossRef]
22. Du, C.; Gao, X.; Kitamura, S. Measures to decrease and utilize steelmaking slag. *J. Sustain. Metall.* **2019**, *5*, 141–153. [CrossRef]
23. Du, C.; Gao, X.; Ueda, S.; Kitamura, S. Separation and recovery of phosphorus from steelmaking slag via a selective leaching–chemical precipitation process. *Hydrometallurgy* **2019**, *189*, 105109. [CrossRef]
24. Lang, Y.; Matsuura, H.; Tsukihashi, F. Long-term dissolution behavior of steelmaking slag and its composite materials in seawater. *J. Sustain. Metall.* **2017**, *3*, 729–736. [CrossRef]
25. Matsuura, H.; Zhang, X.; Zang, L.; Zhang, G.; Tsukihashi, F. Dissolution mechanisms of steelmaking slags in sea water. *Miner. Process Extr. Metall.* **2017**, *126*, 11–21. [CrossRef]
26. Zhang, X.; Atsumi, H.; Matsuura, H.; Tsukihashi, F. Influence of gluconic acid on dissolution of Si, P and Fe from steelmaking slag with different composition into seawater. *ISIJ Int.* **2014**, *54*, 1443–1449. [CrossRef]
27. Diao, J.; Xie, B.; Wang, Y.; Guo, X. Recovery of phosphorus from dephosphorization slag produced by duplex high phosphorus hot metal refining. *ISIJ Int.* **2012**, *52*, 955–959. [CrossRef]
28. Du, C.; Gao, X.; Kim, S.; Ueda, S.; Kitamura, S. Effects of acid and Na_2SiO_3 modification on the dissolution behavior of $2CaO{\cdot}SiO_2$-$3CaO{\cdot}P_2O_5$ solid solution in aqueous solutions. *ISIJ Int.* **2016**, *56*, 1436–1444. [CrossRef]
29. Shu, Q.; Liu, Y. Effects of basicity, MgO and MnO on mineralogical phases of CaO–FeO_x–SiO_2–P_2O_5 slag. *Ironmak. Steelmak.* **2018**, *45*, 363–370. [CrossRef]
30. Li, J.; Zhang, M.; Guo, M.; Yang, X. Phosphate enrichment mechanism in CaO–SiO_2–FeO–Fe_2O_3–P_2O_5 steelmaking slags with lower binary basicity. *Int. J. Miner. Metall. Mater.* **2016**, *23*, 520–533. [CrossRef]
31. Lin, L.; Bao, Y.; Wang, M.; Zhou, H.; Zhang, L. Influence of SiO_2 modification on phosphorus enrichment in P bearing steelmaking slag. *Ironmak. Steelmak.* **2013**, *40*, 521–527. [CrossRef]
32. Lin, L.; Bao, Y.; Wang, M.; Jiang, W.; Zhou, H. Separation and recovery of phosphorus from P-bearing steelmaking slag. *J. Iron Steel Res. Int.* **2014**, *21*, 496–502. [CrossRef]
33. Matsubae-Yokoyama, K.; Kubo, H.; Nagasaka, T. Recycling effects of residual slag after magnetic separation for phosphorus recovery from hot metal dephosphorization slag. *ISIJ Int.* **2010**, *50*, 65–70. [CrossRef]